

Supplementary Information

Ultrathin amorphous α -Co(OH)₂ nanosheets grown
on Ag nanowire surfaces as highly active and
durable electrocatalyst for oxygen evolution reaction

Hyeonghun Kim^a, Youngmin Kim^b, Yuseong Noh^c and Won Bae Kim^{*c}

^a *School of Materials Science and Engineering, Gwangju Institute of Science and Technology (GIST), 123 Cheomdangwagi-ro, Buk-gu, Gwangju, 61005, South Korea.*

^b *Carbon Resources Institute, Korea Research Institute of Chemical Technology (KRICT), 141 Gajeong-ro, Yuseong-gu, Daejeon 305-343, South Korea.*

^c *Department of Chemical Engineering, Pohang University of Science and Technology (POSTECH), 77 Cheongam-ro, Nam-gu, Pohang 37673, South Korea.*

Experimental

Synthesis of Materials

Synthesis of silver nanowires: Silver nanowires (Ag NWs) were prepared via a modified polyol reduction method.¹⁵ At first, 480 mg of AgNO₃ (≥99 %, Sigma-Aldrich) and 490 mg of polyvinylpyrrolidone (PVP, MW ~55,000, Sigma-Aldrich) were dissolved in 160 ml of ethylene glycol (EG, 99.5 %, Junsei) and stirred until a homogeneous solution was formed. With continuous magnetic stirring, 0.8 ml of 4 mM CuCl₂·2H₂O (≥99 %, Sigma-Aldrich) solution in EG was added into the solution for producing seeds, which induce a 1D architecture. Then, the solution was heated to 190 °C, which is slightly below the boiling temperature of EG (198 °C), and maintained at this temperature for 30 min. After cooling the suspension down to room temperature, the products were obtained via centrifugation. To remove PVP and EG completely, the precipitates were washed with ethanol (99.9 %, Sigma-Aldrich) and deionized water (DI, 18 MΩ cm, Millipore) several times. The final products were dispersed in DI.

Synthesis of Ag NW@Co NS: α-Co(OH)₂ nanosheets (Co NSs) were prepared through a hydrolysis process at room temperature.¹⁴ In a suspension consisting of 60 mg of the Ag NW in 20 ml DI, Co(NO₃)₂·6H₂O (≥98 %, Sigma-Aldrich) was added, with different atomic ratios of Co:Ag (0.5:1, 2:1 and 3:1). The hybrid Ag NW@Co NS materials were named Ag NW@Co NS1, Ag NW@Co NS2, and Ag NW@Co NS3, respectively. After a homogeneous suspension was obtained, 1 ml of aqueous NaBH₄ (Sigma-Aldrich, ≥99 %) solution (60 mg ml⁻¹) was injected into the reaction bath drop-wise. After stirring for 2 h, the products were collected through centrifugation and washed with DI several times. The precipitates were dried by a freeze-drying method. A pure Co NS control sample was also synthesized by the same process, without the presence of Ag NWs.

Characterization

The structures and compositions of the materials were analysed by a scanning electron microscope (SEM, JEOL 7300) operated at 5 keV and 20 μA , transmission electron microscope (TEM, Technai G2 F30) operated at 300 keV, and energy-dispersive X-ray spectroscopy (EDX) equipped to the TEM. The crystallographic characteristics were identified by X-ray diffraction (XRD, Rigaku Ru-200B) operated at 40 kV and 100 mA with a Cu $K\alpha$ source. The XRD patterns were recorded in the 2θ range of 5-70 $^\circ$ at a scan rate of 2 $^\circ \text{min}^{-1}$. X-ray absorption spectroscopy (XAS) of Co K edge (7709 eV) was obtained on the 7D beamline of the Pohang Accelerator Laboratory (PLS-II) with a Si double crystal monochromator. The XAS data including X-ray absorption near edge structure (XANES) were processed using ATHENA, which belongs to the IFEFFIT software package.

Electrochemical Measurement

All the electrochemical tests were performed with a three-electrode cell consisting of a catalyst-modified working electrode, a Pt wire as a counter electrode, and a saturated calomel reference electrode (SCE). A rotating disk electrode (RDE) with a diameter of 5 mm was polished with 1, 0.3, and 0.05 μm alumina paste to achieve a glass like surface, and used as the working electrode. A catalyst ink was prepared by dispersing of 3 mg of the catalyst sample and 0.1 ml 5 wt% Nafion ionomer aqueous solution in 0.9 ml of anhydrous ethanol as a solvent and 10 μl of the ink, which corresponds to 0.153 mg cm^{-2} , and was loaded uniformly on the RDE. An N_2 purged 1 M KOH was used as the electrolyte for all the tests. Cyclic voltammetry scans (CVs) were performed at a scan rate of 50 mV s^{-1} in the range of -0.2 to 0.5 V (vs. SCE) and linear sweep voltammograms (LSVs) were measured at a scan rate of 10 mV s^{-1} from 0.1 to 0.7 V (vs.

SCE) after operating five CV cycles.^{S4-10} All the LSV polarization curves were IR correlated based on the ohmic law by considering a solution resistance that was estimated through electrochemical impedance spectroscopy (EIS) measurements. EIS measurements were conducted at 0.55 V (vs. SCE) with a frequency range of 10 kHz to 0.01 Hz by applying an AC amplitude of 5 mV. Chronopotentiometry tests at a fixed current density (10 mA cm⁻²) were conducted for 10 h to compare catalytic durability under suitable conditions. During the measurements, the RDE was rotated at a rate of 1600 rpm to increase the mass transfer of the oxygen bubbles released. All the measurements were operated by Autolab PGSTAT30 (Eco Chemie) and the potential was plotted against the reversible hydrogen electrode (RHE). For determining an onset overpotential, a baseline was calculated by linear fitting in a range of non-faradaic region (1.2-1.4 V (vs. RHE)) and found a voltage, which is initially off the baseline, as the onset point.

Intrinsic activities of the catalysts were compared on the basis of turnover frequencies (TOFs) at overpotentials of 300 or 350 mV. The TOF was calculated based on the following equation:

$$\text{TOF} = \text{JA} / 4Fm$$

where J is the current density measured at the overpotentials (A cm⁻²), A is the geometric area of the RDE (0.196 cm²), F is the Faraday constant (96485 C mol⁻¹), and m is the number of moles of active elements in the modified electrode. Because of insignificant OER activity of silver at the given overpotentials, only the Co species were regarded as active sites. The calculation is accomplished based on an assumption that all of the Co species participated in the reaction as active sites.^{10,11, S1-3, S14,S15}

Table S1. Molar ratio (Co/Ag) of the Ag NW@Co NSs estimated from EDX

	Ag NW@Co NS1	Ag NW@Co NS2	Ag NW@Co NS3
Molar ratio of added precursors (Co/Ag)	0.5/1	2/1	3/1
Measured molar ratio from EDX (Co/Ag)	0.42/1	2.22/1	2.80/1

Table S2. Comparison of the OER performances with different catalysts.

	Ag NW@ Co NS1	Ag NW@ Co NS2	Ag NW@ Co NS3	Co NS	Ag NW+ Co NS
Co loading ($\mu\text{g cm}^{-2}$)	29.2	61.4	70.0	68.0	68.0
Onset (V vs. RHE)	-	1.45	1.45	1.55	1.45
E_{10} (V vs. RHE)	1.67	1.56	1.55	1.63	1.57
Overpotential (η_{10} , mV)	440	330	320	400	340
TOF (s^{-1}) at $\eta=300$	-	0.011	0.016	0.0016	0.0089
TOF (s^{-1}) at $\eta=350$	-	0.044	0.053	0.0061	0.031

Table S3. Comparison of the OER performances with recently reported catalysts.

	E_{10} (V vs. RHE)	TOF (s^{-1}) at $\eta=300$ mV	TOF (s^{-1}) at $\eta=350$ mV	Ref.
Ag NW@Co NS3	1.55	0.016	0.053	This work
NiCo-NS	1.56	0.01	-	10
CoCo-NS	1.58	0.003	-	10
HCO-NHSs	1.57	-	-	11
NiCo-LDH	1.65	-	0.002 at $\eta=419$ mV	S1
Co-CoO/N-rGO	1.62	-	-	S2
Co monolayer	1.62 (without iR-correction)	-	2.13 at $\eta=400$ mV	S3
Au@Co ₃ O ₄	-	-	0.015	S11
Ni _{0.6} Fe _{0.4} film on Au substrate	1.51	0.80	-	S12
Ni-Fe-oxy(hydroxide)/borate	-	-	1.4 at $\eta=400$ mV	S13

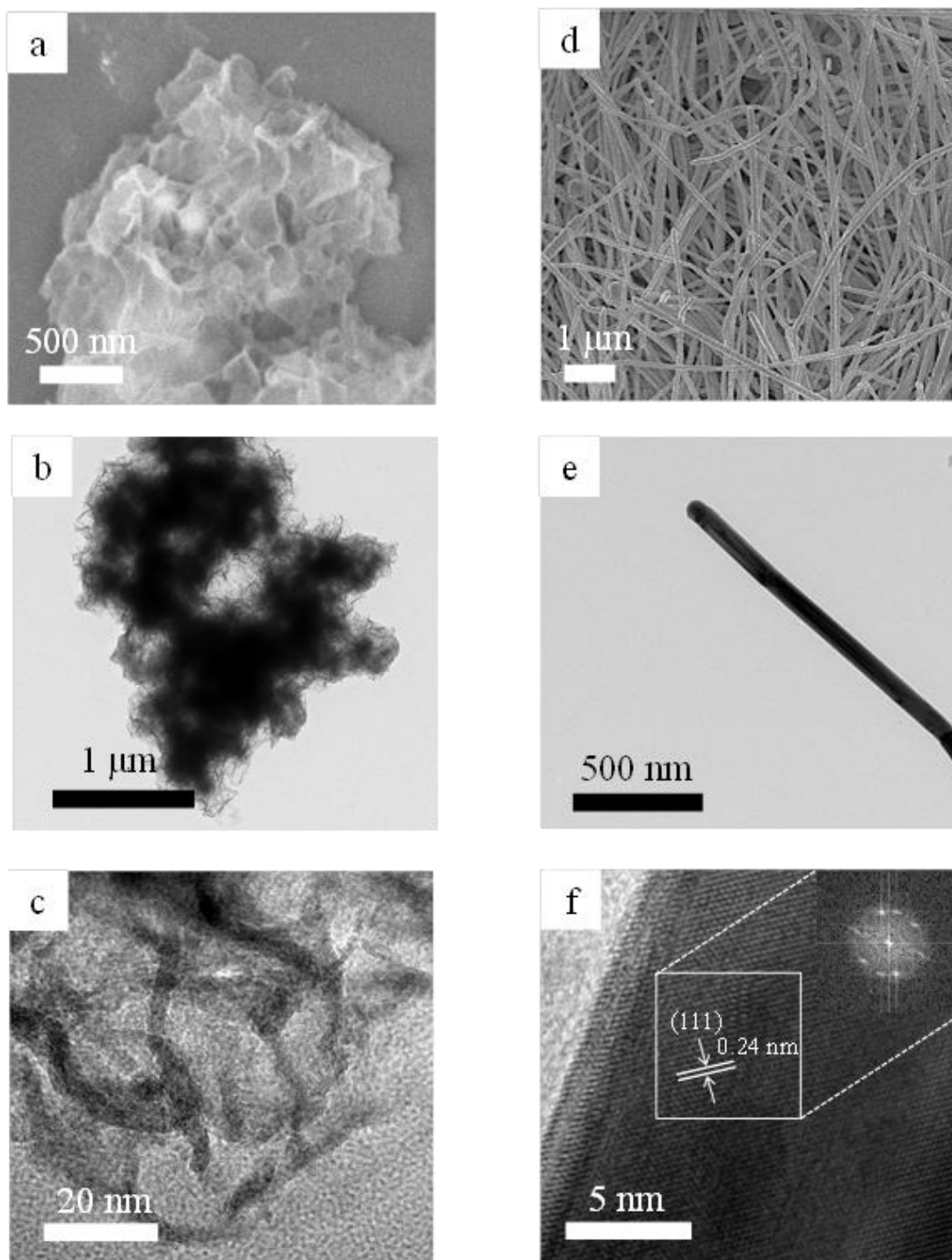


Figure S1. (a) SEM, (b) TEM and (c) HRTEM images of the pure Co NS. (d) SEM and (e) TEM and (f) HRTEM images of the Ag NW. The inset of panel (f) represents FFT pattern from the selected region.

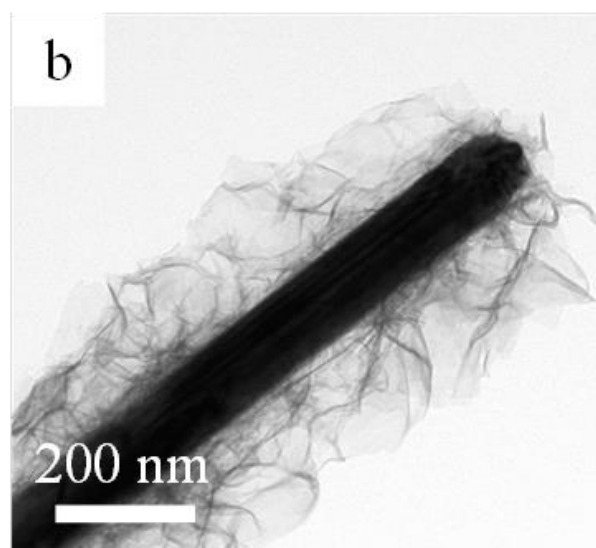
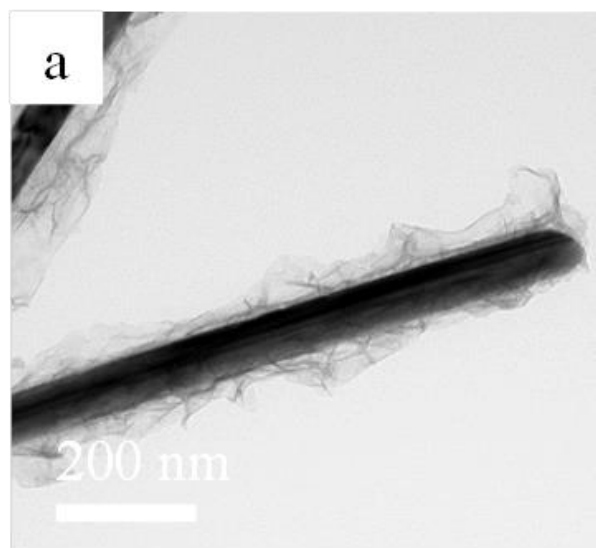


Figure S2. TEM images of (a) the Ag NW@Co NS1 and (b) Ag NW@Co NS2.

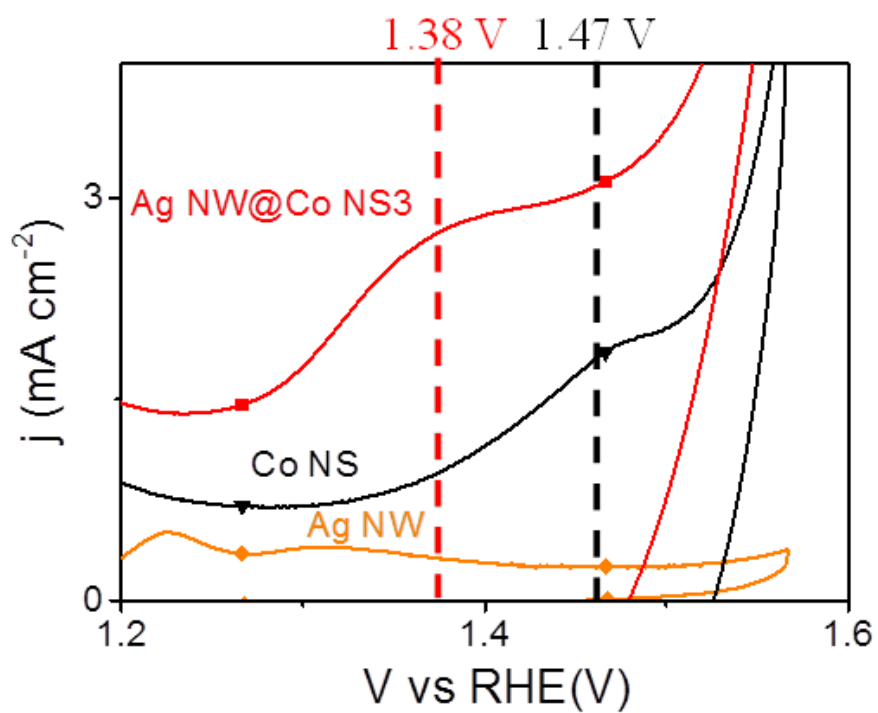


Figure S3. CVs of the Ag NW@Co NS3, pure Co NS and Ag NW catalysts in an N_2 -saturated 1 M KOH electrolyte at a scan rate of 50 mV s^{-1} .

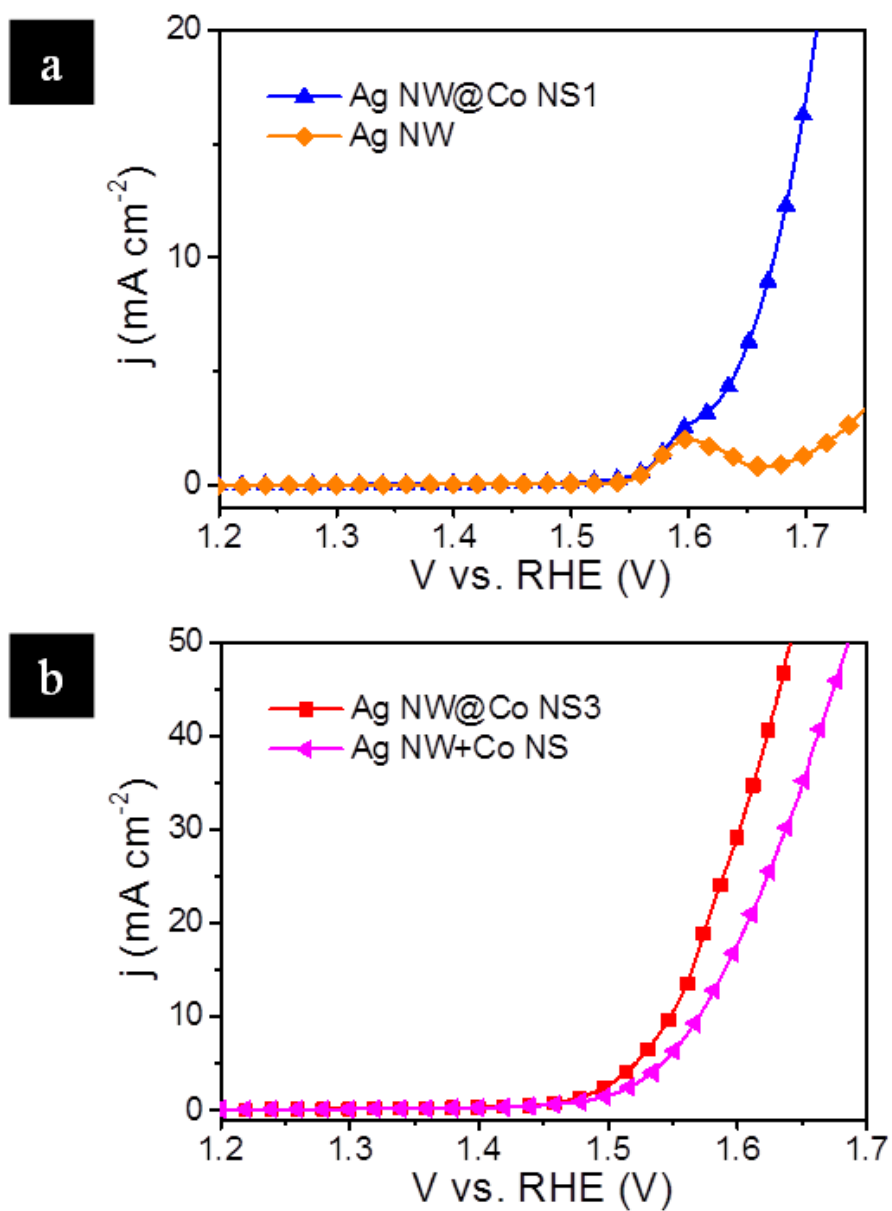


Figure S4. LSVs of (a) the Ag NW@Co NS1 and Ag NW and (b) Ag NW@Co NS 3 and physically mixed sample (Ag NW+Co NS) in an N_2 -saturated 1 M KOH electrolyte at a rotation rate of 1600 rpm and a scan rate of 10 mV s^{-1} .

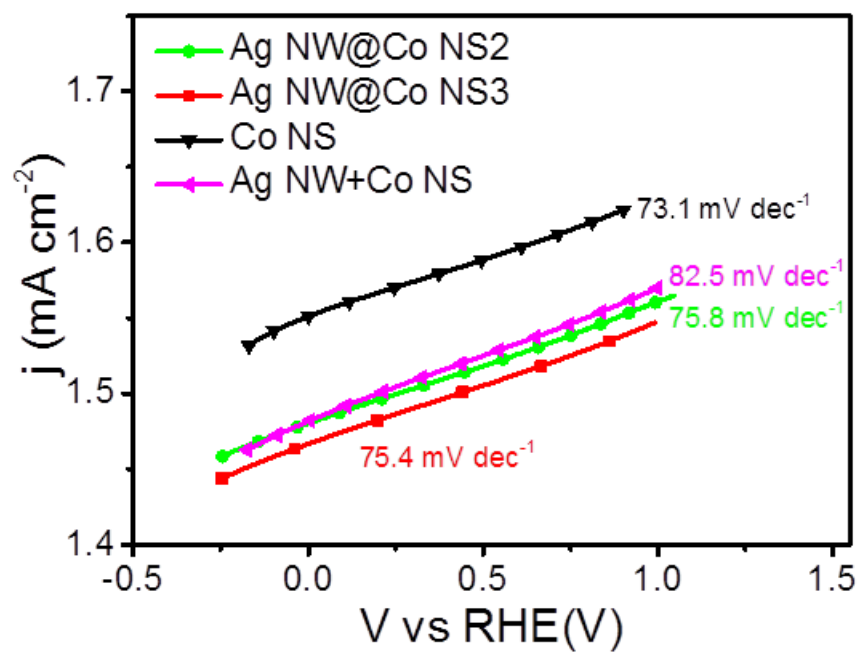


Figure S5. Tafel plots of the Ag NW@Co NS2 and 3, pure Co NS and physically mixed sample (Ag NW+Co NS).

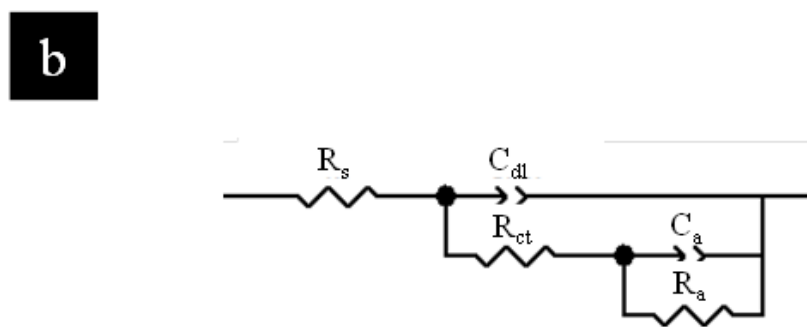
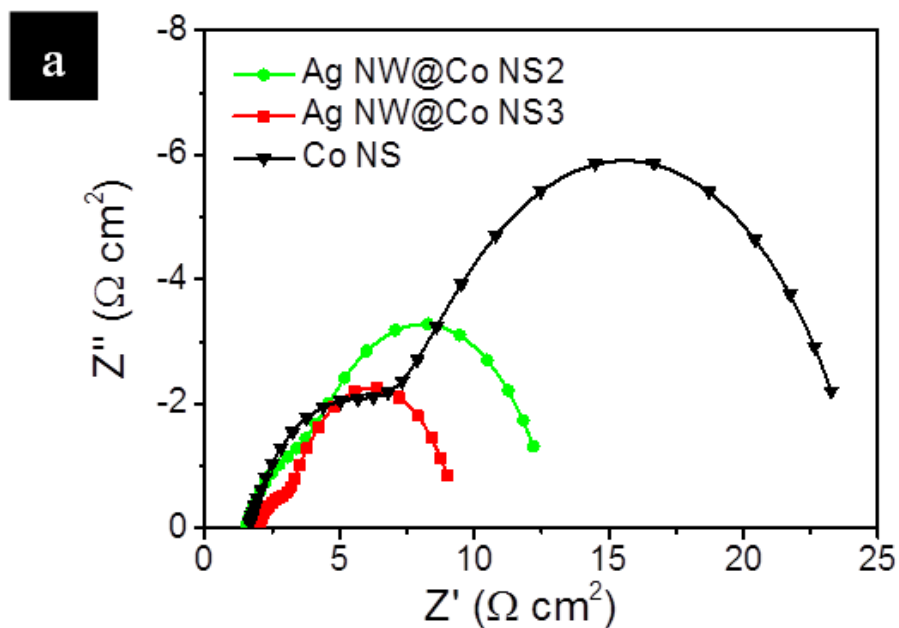


Figure S6. (a) Nyquist plots of the Ag NW@Co NS2 and 3 and pure Co NS. (b) Electrical equivalent circuit, which R_s is the uncompensated ohmic resistance, R_{ct} is the charge transfer resistance, R_a the adsorption resistance, C_{dl} is the double-layer capacitance and C_a is the pseudo-capacitance coming from the adsorption of electrolytes. For modeling more exactly, constant phase elements (CPE) were used instead of the capacitances because of the non-uniformity of surface reaction sites.

References

- S1. J. Jiang, A. Zhang, L. Li and L. Ai, *J. Power Sources*, 2015, **278**, 445-451.
- S2. X. Liu, W. Liu, M. Ko, M. Park, M. G. Kim, P. Oh, S. Chae, S. Park, A. Casimir, G. Wu and J. Cho, *Adv. Funct. Mater.*, 2015, **25**, 5799-5808.
- S3. L. Wu, Q. Li, C. H. Wu, H. Zhu, A. M.-Garcia, B. Shen, J. Guo and S. Sun, *J. Am. Chem. Soc.*, 2015, **137**, 7071-7074.
- S4. J. Masa, P. Weide, D. Peeters, I. Sinev, W. Xia, Z. Sun, C. Somsen, M. Muhler and W. Schuhmann, *Adv. Energy Mater.*, 2016, **6**, 1502313-1502322.
- S5. H. Wang, H.-W. Lee, Y. Deng, Z. Liu, P.-C. Hsu, Y. Liu, D. Lin and Y. Cui, *Nat. Commun.*, 2015, **6**, 7261.
- S6. C. Zhang, M. Antonietti and T.-P. Fellingner, *Adv. Funct. Mater.*, 2014, **24**, 7655-7665.
- S7. Y. Su, Y. Zhu, H. Jiang, J. Shen, X. Yang, W. Xou, J. Chen and C. Li, *Nanoscale*, 2014, **6**, 15080-15089.
- S8. S. Mao, Z. Wen, T. Huang, Y. Hou and J. Chen, *Energy Environ. Sci.*, 2014, **7**, 609-616.
- S9. Y. Zhao, B. Sun, X. Huang, H. Liu, D. Su, K. Sun and G. Wang, *J. Mater. Chem. A*, 2015, **3**, 5402-5408.
- S10. X. Zhou, Z. Xia, Z. Tian, Y. Ma and Y. Qu, *J. Mater. Chem. A*, 2015, **3**, 8107-8114.
- S11. Z. Zhuang, W. Sheng and Y. Yan, *Adv. Mater.*, 2014, **26**, 3950-3955.
- S12. M. W. Louie and A. T. Bell, *J. Am. Chem. Soc.*, 2013, **135**, 12329-12337.
- S13. A. M. Smith, L. Trotochaud, M. S. Burke and S. W. Boettcher, *Chem. Commun.*, 2015, **51**, 5261-5263.
- S14. F. Song and X. Hu, *J. Am. Chem. Soc.*, 2014, **136**, 16481-16484.

S15. J. Huang, J. Chen, T. Yao, J. He, S. Jiang, Z. Sun, Q. Liu, W. Cheng, F. Hu, Y. Jinag, Z. Pan and S. Wei, *Angew. Chem. Int. Ed.*, 2015, **54**, 8722-8727.